UNIVERSITY OF THE WITWATERSRAND, JOHANNESBURG

SCHOOL OF MECHANICAL, INDUSTRIAL & AERONAUTICAL ENGINEERING

MECN4029A - Mechatronics II

Project Assignment

Group 9

Project B – Solar Tracker

1706998 - Oratile Megalane

2333287 - Shipakane Ndhlovu

2435550 - Sagale Sodi

2525482 - Ashley Muzika

UNIVERSITY OF THE WITWATERSRAND, JOHANNESBURG

SCHOOL OF MECHANICAL, INDUSTRIAL & AERONAUTICAL ENGINEERING

Disclosure – Use of Artificial-Intelligence (AI) Generated Content

2024

Students must acknowledge all use of AI.

Select all applicable statements and complete sections 2, 3, 4 and 5 if applicable.

1. Disclosure: No AI use

☒ I acknowledge that no AI tools/technologies (Grammarly, ChatGPT, Bard, Quillbot, OpenAI etc) were used in the completion of this assessment.

☒ ***I declare that the disclosure is complete and truthful.***

Student number: 2435550 1706998 2333287 2525482

Course code: MECN4029A

Date: 19/05/2024

Executive Summary

The design of a solar tracker system was undertaken following the observation of increased power insecurity in and around Johannesburg. Load shedding, among numerous municipal power outages has necessitated the use of off-grid power for companies, institutions, and households. Among the most affected groups by power outages are students living in the city of Johannesburg and residing in residences in and around the University of the Witwatersrand Campus. This has resulted in increased demand for solutions during power crises. A student friendly, off-grid device or system is required to equip students with the necessary access to power to charge laptops and electronic devices in the case of sudden outages. This problem scenario was the basis for the development of an optimised solar bench design, similar to existing solar benches used in institutions like Wits University. It was determined that to maximise power generation for increased use, the bench could be modified by introducing a moveable solar panel that tracks the sun's positions during the day. The system was as such required to effectively track the sun's position throughout the year. Models were developed for extreme cases where the sun spent the longest time in the sky at higher elevation angles (summer) and where the sun spent a shorter amount of time at lower elevation angles (winter). The performance parameters were defined for the panel to ensure a system that was stable, could respond to a sudden input as well as withstand disturbances. An overshoot of no more than 0% was required, with a peak time and settling time around 10 seconds and 20 seconds respectively. These parameters were selected to minimise noise levels, limit instability and achieve a near accurate response to the position input. The equations of motion of the system were derived by analysing the 3 major aspects of the system – electrical, mechanical and electromechanical. The final equation of motion relates the motion of the panel to an input voltage through the torque produced by a motor. The mathematical model was linearised and using both analytical and simulation methods. The linear model was used as the basis for controller design. The controller designs were completed through an iterative process to achieve the best possible results to meet the set performance parameters while considering limitations.

The final solar tracer system closely tracks the sun's position using PI and root locus controllers for both summer and winter seasons. It can withstand sudden disturbances caused by wind or a sudden impact.

Contents

List of Figures

List of Tables

1. Introduction

1.1. Problem Background

The use of solar energy as an alternative power source for off grid use has grown rapidly in South Africa, largely due to increased periods of load shedding and power outages. This necessitates the introduction of solar powered systems in several industries and institutions. The University of the Witwatersrand is one such institution that has implemented the use of solar energy for alternative power supply.

The use of solar energy has been introduced through mobile solar benches. The solar bench is depicted in Figure 1. The solar benches provide students with off-grid electricity in the case of a power outage in the university.

Figure 1: Solar Bench

Following recent power outages and further electricity insecurity in and around Braamfontein, institutions would greatly benefit from the increased use of off-grid electricity to provide students the ability to continue powering their devices. An increase in output would be required to match the possible increased use of the solar bench during power outages.

Observing that the solar system panel is stationary, it doesn't have the capability to capture available maximum solar energy. This is due to the sun moving throughout the day and throughout seasons. In that regard less sun light is exposed to the surface area of the panel due

to its orientation in relation to sun position. Therefore, there is a need to maximum the solar energy stored by ensuring that the panel is orientated to absorb maximum possible solar energy.

Observing the scenario and problem at present, being the need to design a solar system that capture maximum solar energy for student use through the night as there is no solar energy during the night. It was proposed to develop solar tracking solar panel that can track the sun's trajectory to ensure maximum light is captured during the day. In that regard control system of the solar tracking system is required to ensure the possibility of this. The use of a solar tracking system is costly need to purchase, implement and maintain the system which is observed as financial problem. In that regard it was proposed that the control and solar tracking system needed to solve the problem, must have lowest cost possible. This was proposed under the concern of future possible outages in Braamfontein over long durations. In that regard the solar bench design will encompass operations and requirements drawn from these other application affected by the problem.

1.2. Objectives

- Develop a model of a solar tracker that tracks the sun's position.
- Develop a control for the solar tracking system with real time data.

1.3. Design Considerations

The design of the solar tracker should consider the type of application and users. The users and context of application will affect the desired performance specifications and should thus be evaluated.

Application:

- The current output voltage of the solar bench, as taken from the output of a similar solar bench on the market is 120 V [1]

1.4. Performance Specifications

Table 1: Performance Specifications

Parameter	**Value**
Rise time [s]	$2 < t_r < 10$
Settling time [s]	$t_s < 20$
Overshoot [%]	0 %
Steady State Error [rad]	0
Bandwidth	

These performance parameters are drafted from observing how the system is expected to track the sun while ensuring that the structural integrity and safety of the student's is kept. It should be noted that theses values are based of judgement that came about inspection of the panel and its rotating mechanisms. This involves not having a short settling time, due to this resulting in fast rotation of the panel due to safety concerns. The rise time was expected to be less due expected to be short to reduce high dynamic loading on the structure of the panel.

2. System Parameters and Modelling

As the system is expected to maximise exposure of sun radiation on the panel surface by tracking the sun. In that regard the movement of the sun becomes a parameter of interest to this problem. Whereby the sun was observed to be moving from east to west daily and move from north to south seasonally [1]. Translating the sun's motion to the panel's expected motion, it can be noted that the zenith axis aligns the suns daily movement, and the azimuth aligns with the season motion as observed in Figure 2.

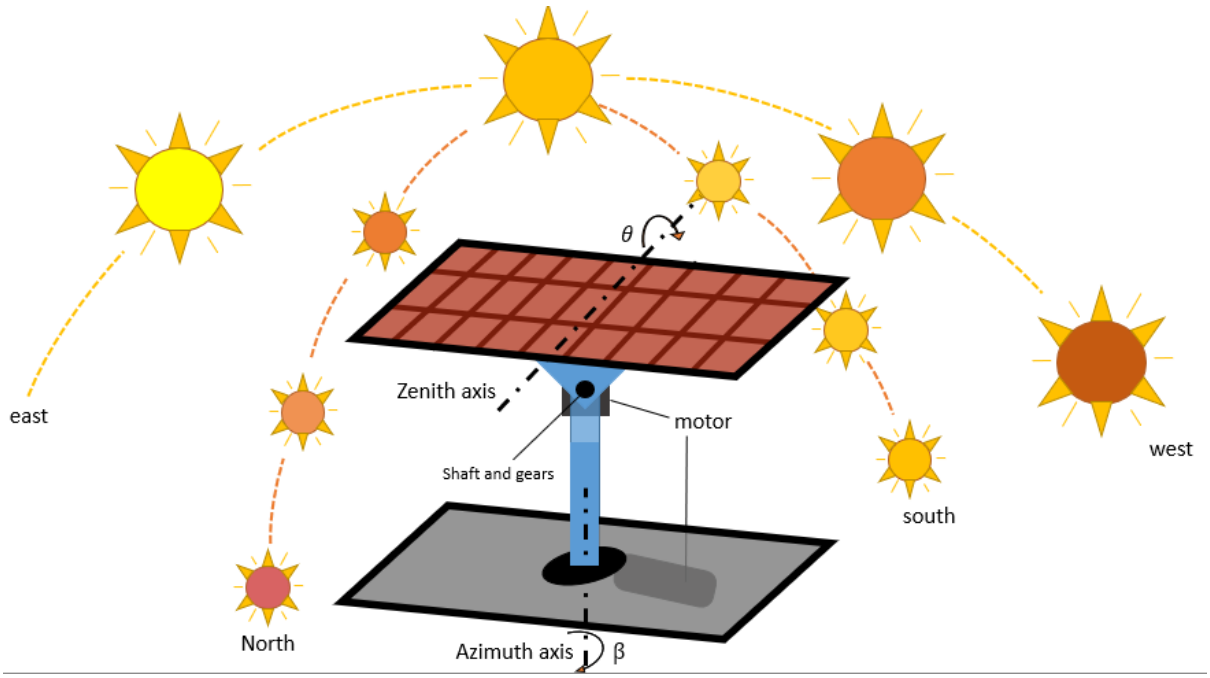

Figure 2: Simplified Solar Model

Observing the change in motion of the sun in the azimuth axis, it shows that the sun will raise and set at different times during the day hence causing variable sun ray incident interval. This will be further accounted for in the modelling of the tracking system. The approach towards

the tracking sun's position was compared with a direct and indirect way. Whereby the direct approach involves using the concept of photocell, which measures change in resistance along the photocell to identify the sun's location. By rotating the panel until the change in resistance along the panel is close to zero [2].

The indirect approach involves using published data of the sun's positions with respect to an observer in Braamfontein. As the sun's position for each day from 2023 1 January – 31 December relative to coordinates of the university of Witwatersrand will be captured and used as inputs of interest to the scenario. When developing the panel's model.

It was decided that the approach that will suffice for this design, is the use of published data. This is primarily due to considering the use of a photocell which will require an algorithm and hence being costly compared to the use of published and peer reviewed data. The direct approach is costly due the complexity it causes with the addition of using a photocell in tracking and the complexity inherently increases the cost due to factors such cost function of each component when observing both approaches. In that regard the published data was settled on and observed in the appendix A.

2.1. Physical Model

Observing the problem on an overview perspective, it is the developing a system to enable an initially stationary solar panel track the sun. For this to occur the panel needs to be updated with components that will allow it to track the sun. From application practice, it was observed that the overall systems consist of electrical, electromagnetic and mechanical components to ensure the establishment of the proposed solution. Figure 3 shows the schematic of the physical model.

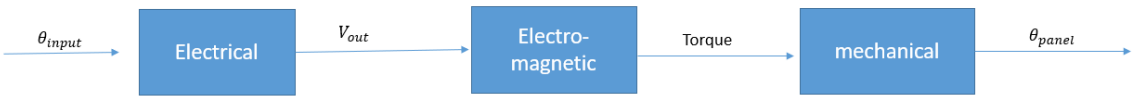

Figure 3: Open-Loop Physical Model.

After investigating how to integrate the categories of expected components needed to for the design, Figure 3 was established. Which shows an input signal of θ_{input} which is the required angular displacement needed for the panel from the outsourced sun position data. This is signal

is feed as input in the electrical part of the system, which will convert its input signal to a voltage using a potentiometer or variable resistor. This is due to the electromagnetic part not being able to read an angle signal but can read a voltage signal. Which is why the output of the electrical is a voltage signal that is fed as input signal in the electromagnetic part.

The electromagnetic part enables actuation on the mechanical part (plant) based of its input volage signal. The output of the electromagnetic part is a torque based of its input voltage signal, as this torque becomes an input in the mechanical part. Which there after the panel moves resulting in a θ_{output}. The system presented in Figure 3 shows that the system can perform what is required, which is track the sun based on the analysis around it but how well it tracks the sun becomes a problem.

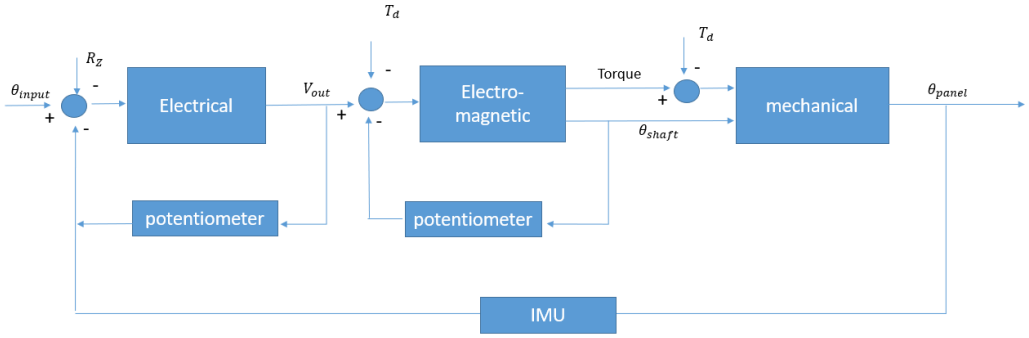

Figure 4: Closed-Loop Physical Model

After observing the incompetency of the model in Figure 3, the closed loop system shown in Figure 4 was established as a better version of the open loop in Figure 3. Whereby it accounts for measuring the panel's location with respect to θ_{input} through the addition of a feedback. As compensator was seen inadequate due presence of possible expected disturbances to the system resulting randomness in the output, which were friction (gear and shaft) and wind. In that regard, the closed loop is a version of the open loop that is robust and ensure that the θ_{output} meets the expected θ_{input} despite anchoring losses in the component categories that cause deviation on θ_{output}.

2.2 Hardware

2.2.1 Solar Panel

Table 2 summarizes the specifications of the solar panels that were analysed.

Table 2: Solar panel specifications

Specification	Value
Output Power	12kW
Length	3.40 m
Width	1.84 m
Mass	76.0 kg
Distance to axis of rotation(y)	0.20 m
Power output	1.20 kW

2.2.3 Motor and gearbox

The specifications are motor and gearbox combination are shown in Table 3.

Table 3: Motor and Gearbox specifications

Specification	Value
Nominal voltage	12.0 V
Nominal current	10.0 A
Nominal torque	0.59 Nm
Maximum torque	6.06 Nm
Torque constant (K_t)	0.067 Nm/A
Armature resistance (R_a)	0.214 Ω
Armature inductance (L_a)	1.5 mH
Gear ratio (n)	35

2.1.1. Assumptions

The following assumptions and approximations were made in coming up with design of the system:

- The displacements on the potentiometer are directly proportional to resistance.
- The motor operates in the linear operating range of the motor.
- The motor impedance and the back emf remains constant throughout the operation.
- There were no switching delays or losses in the motor.
- There was zero sliding friction between the gears therefore rigid body dynamics were applied.

- Aerodynamics forces were neglected due to the low angular velocities of the solar panel.
- The mass of the panel was concentrated at the centroid of the solar panel.

2.2. Mathematical Model

The mathematical model was established with consideration of the component's selection drawn from Figure 4 and with the incorporation of Figure 5. The development of each sub system's governing equation was developed using newton's law (mechanical and electromagnetic) and the consideration of Kirchoff's law (electrical and electromagnetic). The governing equations of the entire system was done with the aid of dimensional analysis and the theory of superposition of the variable that interact between sub-section such as T_m and e_a.

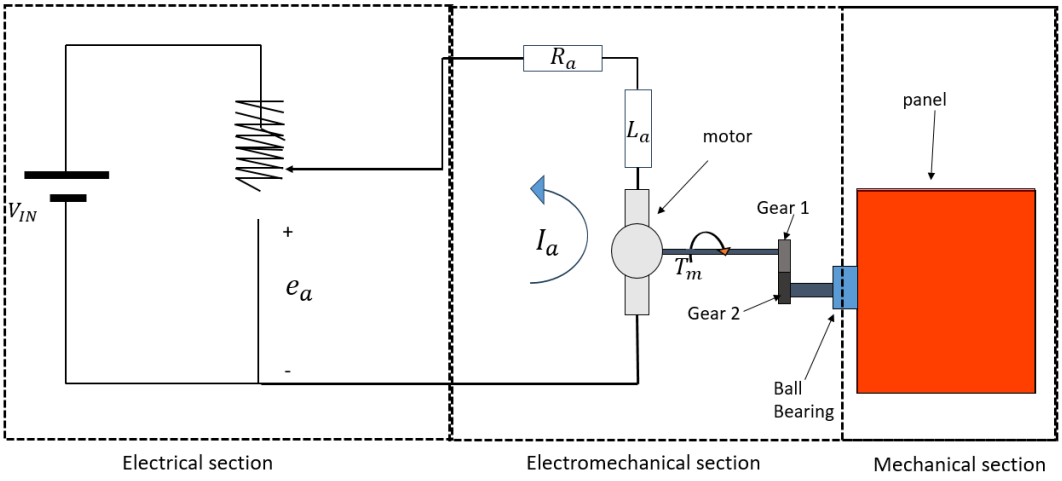

Figure 5 Figure showing the schematic of the physical mode [2].

Electrical Components:

The electrical section involves the use of a potentiometer that is to be used to convert the signal from the input which is rotation into a voltage drop. Whereby the potentiometer can be observed as a variable resistor [c]

The voltage across the motor is:

$$e_a = V_{in}\,\theta_1 \qquad (1)$$

where θ_1 is the relative displacement of the potentiometer. This is the reference (input) in the physical system.

Electromagnetic components:

The electromagnetic section involves the use of a DC motor that is transmits the voltage signal from the electrical section into a torque to the mechanical part through gears.

Using Kirchoff's voltage law:

$$e_a = R_a + L_a\left(\frac{di_a}{dt}\right) + e_m \quad (2)$$

where e_m is the back emf of the motor which is equivalent to:

$$e_m = k_e\dot{\theta}_a \quad (3)$$

Where θ_a is the angle of rotation of the motor. The torque produced by the motor is determined using equation 4.

$$T(t)=k_t i\ (t) \quad (4)$$

Where k_t is the motor torque constant. Substituting equations 3 and 4 into equation 2 to eliminate i(t).

$$e_a\ (t)= \frac{R_a}{k_t}T_a(t) + \frac{R_a}{k_t}\frac{d}{dt}\dot{(T_a)}(t) + k_e\dot{\theta}_a(t) \quad (5)$$

Mechanical Components:

The mechanical part of the system involves the physical panel structure and panel itself. Whereby the load experienced by this part of the system is received through gears that transmit the torque from the electromagnetic section.

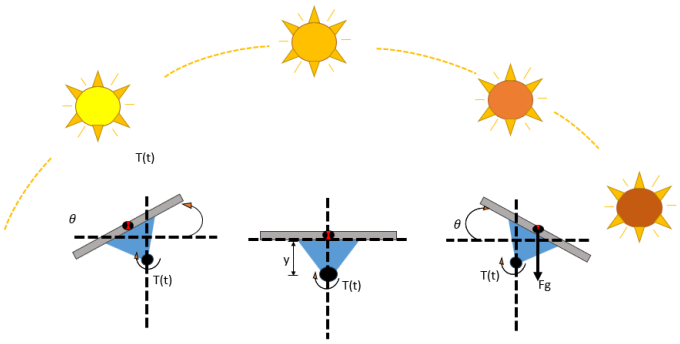

Figure 6: Panel Motion

From Figure 6, using Newton's second law of motion, the rotational acceleration of the panel is modelled using equation 8:

$$T_b = nT_a \tag{6}$$

$$\dot{\theta_a} = n\dot{\theta}_b \tag{7}$$

$$J\ddot{\theta_b} = T_b(t) + mgysin\theta_b - c\dot{\theta}_b \tag{8}$$

Where n is the gear ratio, c is the damping coefficient, J is the moment of inertia of the panel. Combining equations 1 to 8, the nonlinear model of the system is defined by:

$$J\ddot{\theta_a} = \frac{nk_tV_{in}}{R_a}\theta_1 - n^2\dot{T_a} - \frac{k_tk_e}{R_a}\theta_a + mgysin\theta_a - c\dot{\theta_a} \tag{9}$$

From equation 4:

$$\dot{T_a} = k_t \frac{di_a}{dt} \tag{10}$$

From equation 2:

$$\frac{di_a}{dt} = \frac{k_tV_{in}}{R_aL_a}\theta_1 - \frac{R_a}{L_a} - \frac{k_e}{L_a}\theta_a \tag{11}$$

Substituting equation 10 and 11 in equation 9 gives:

$$J\ddot{\theta_a} = \frac{nk_tV_{in}}{R_a}\theta_1 - n^2\left(k_t\left(\frac{k_tV_{in}}{R_aL_a}\theta_1 - \frac{R_a}{L_a} - \frac{k_e}{L_a}\theta_a\right)\right) - \frac{k_tk_e}{R_a}\theta_a + mgysin\theta_a - c\dot{\theta_a} \tag{12}$$

$$J\ddot{\theta_a} = \left(\frac{nk_tV_{in}}{R_a} - \frac{n^2{k_t}^2V_{in}}{R_aL_a}\right)\theta_1 + \left(\frac{n^2k_tk_e}{L_a} - \frac{k_tk_e}{R_a}\right)\theta_a + mgysin\theta_a - c\dot{\theta_a} + \frac{n^2k_tR_a}{L_a} \tag{13}$$

2.2.1. Linearization

To linearize the equation, the system was approximated to be stable about the point $\theta_1 = \theta_a = 0$. Equation 14 is the linear approximation of the system.

$$J\ddot{\theta_a} = \left(\frac{nk_tV_{in}}{R_a} - \frac{n^2{k_t}^2V_{in}}{R_aL_a}\right)\theta_1 + \left(\frac{n^2k_tk_e}{L_a} - \frac{k_tk_e}{R_a}\right)\theta_a + mgy\theta_a - c\dot{\theta_a} + \frac{n^2k_tR_a}{L_a} \tag{14}$$

2.2.2 Transfer Function

The transfer function calculated the linearized equation 14. The coefficients of all the variables were constants, the following simplification was done to determine the transfer function:

$$A= \frac{\left(\frac{nk_tV_{in}}{R_a} - \frac{n^2{k_t}^2V_{in}}{R_aL_a}\right)}{J} \quad (15)$$

$$B= \frac{\left(\frac{n^2k_tk_e}{L_a} - \frac{k_tk_e}{R_a}\right) + mgy}{J} \quad (16)$$

$$D = \frac{n^2k_tR_a}{JL_a} \quad (17)$$

$$\ddot{\theta_a} = A\theta_1 + B\theta_a - c\dot{\theta_a} + D \quad (14)$$

Using Laplace on both sides of equation 14 assuming that initial conditions are zero:

$$s^2\theta_a(s) = A\theta_1(s) + B\theta_a(s) - s\theta_a(s) + \frac{D}{s} \quad (15)$$

Replacing the constants with the actual values and regrouping the terms gives:

$$\frac{\theta_a}{\theta_1} = \frac{774.4}{s^3+142.7s^2+85.6s+301.1} \quad (16)$$

3. System Dynamic Behaviour

3.1. System Response

Analysing the performance of an uncontrolled system in both the time and frequency domains provides a comprehensive understanding of the system's dynamics and behaviour. The performance of the uncontrolled system in time and frequency response was analysed using the Simulink model shown in Figure 7. Figure 8 shows the subsystem of the Simulink model.

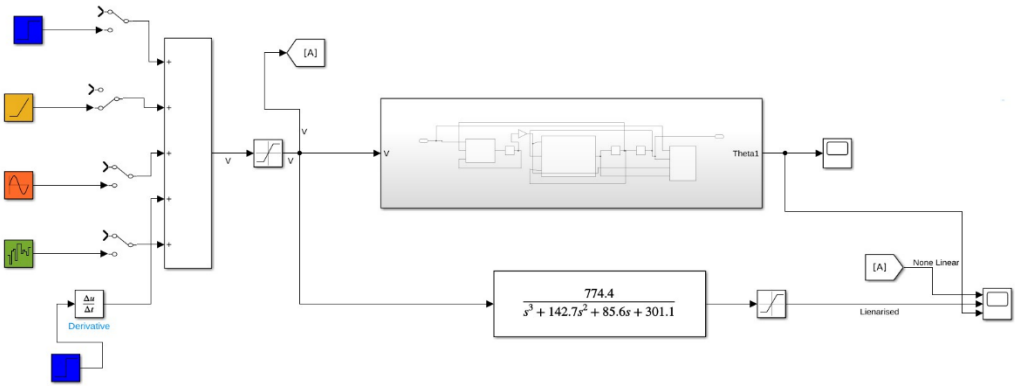

Figure 7:Simulink Model

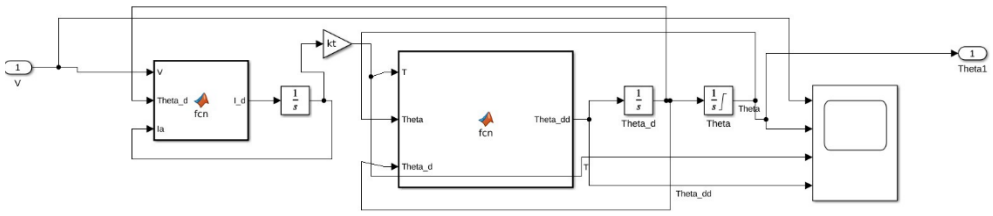

Figure 8:Subsystem of the model.

The system response of the linear and the non-linear response to different inputs is in Figures 9 to 13.

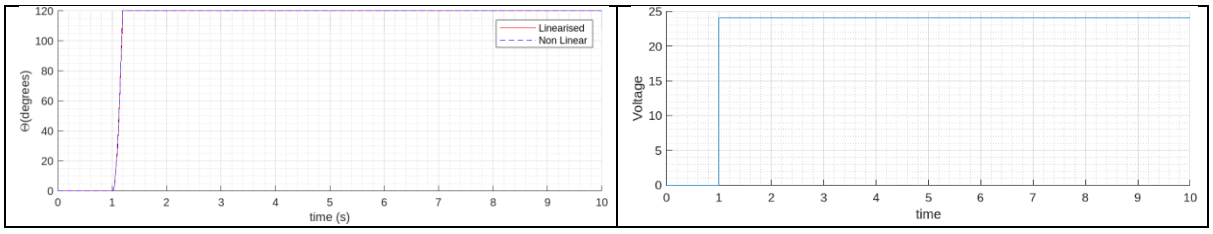

Figure 9: System response to step input.

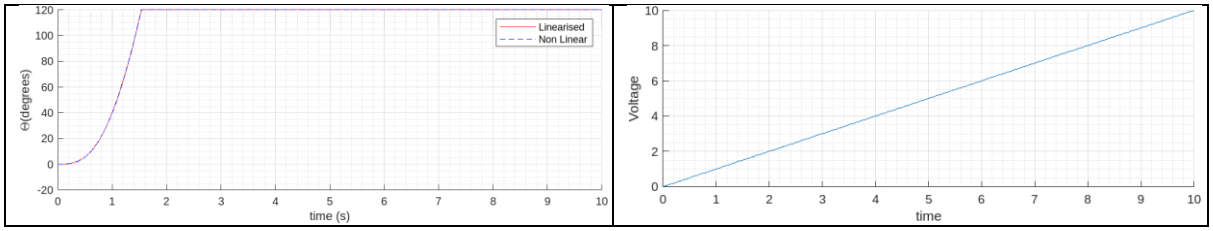

Figure 10:System response to a ramp input.

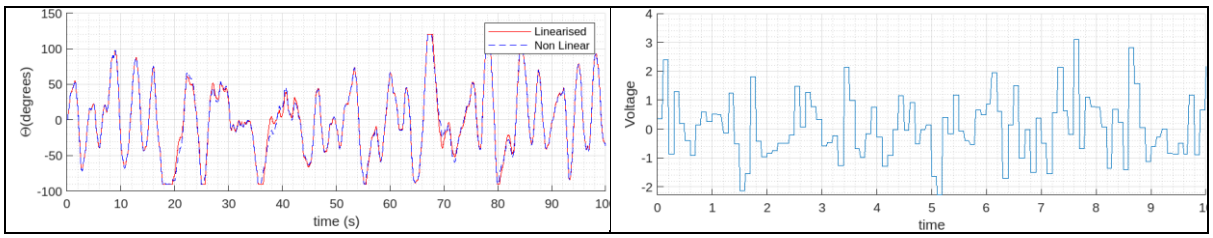

Figure 11:System response to Band Limited White Noise.

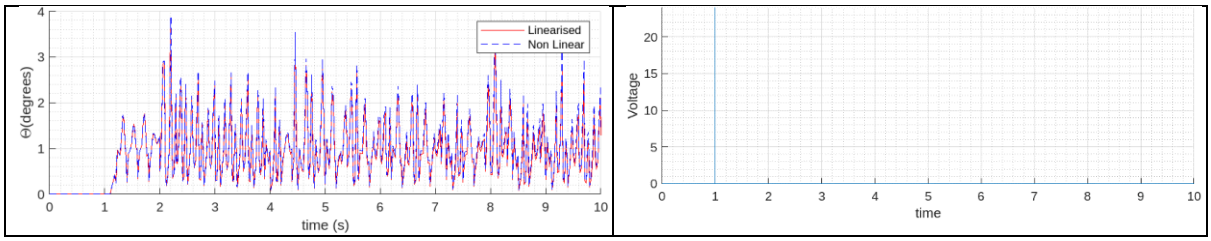

Figure 12: System response to Impulse input.

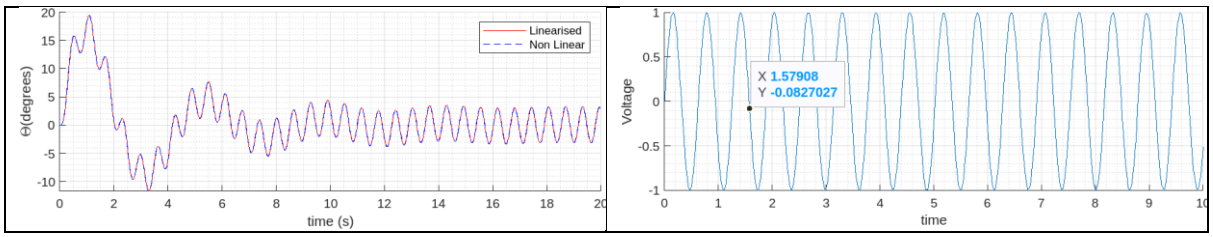

Figure 13:Frequency Response

Figure 9 to 13 shows the correspondence of the linear and nonlinear responses. This was a confirmation that the linearization was done correctly. Comparing the frequency and time responses, it can be concluded that the systems reach a steady state in 1.5 seconds whereas in frequency response the system keeps on oscillating.

3.2. Stability Analysis

The stability of the system was analysed numerically and analytically. The system stability is crucial as it informs the ability of a system to maintain its behaviour in the presence of a disturbance. The system should possess stability in its uncontrolled form as well as it's controlled from.

3.2.1. Analytical Stability Analysis

The transfer function for the uncontrolled system inn equation 16 was used to assess the systems stability.

$$TF = \frac{774.4}{s^3+142.7s^2+85.6s+301.1} \quad (17)$$

The characteristic polynomial is thus given by:

$$s^3 + 142.7s^2 + 85.6s + 301.1 = 0 \quad (18)$$

The roots of the characteristic polynomial are:

$$-142 + 0i$$

$$-0.29 \pm 0.143i$$

The presence of negative real roots with no positive roots indicates the stability of the system. This means that the poles in the s-plane lie on the left-hand side of the imaginary axis. This is an ideal characteristic for the system as it ensures that the system can settle or return to its initial state after a disturbance. Such disturbances like wind and impact from foreign objects should be tolerable by the system.

3.2.2. Numerical Methods – Stability

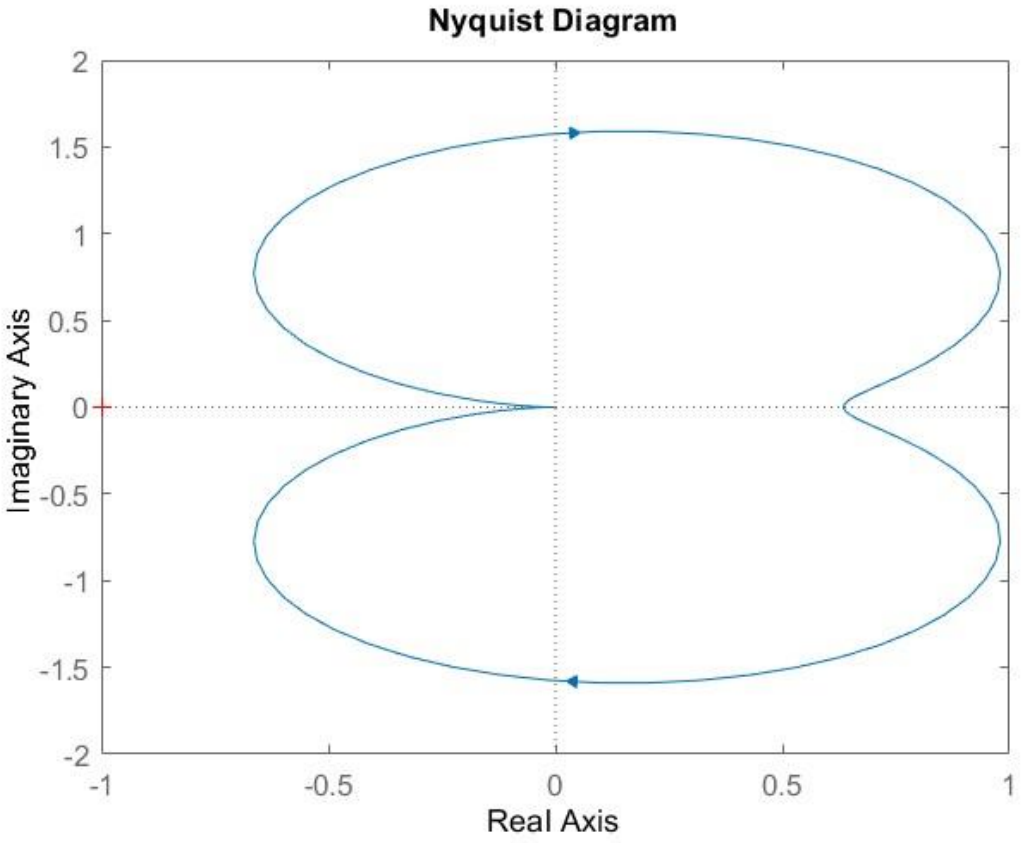

Figure 14:Nyquist Plot

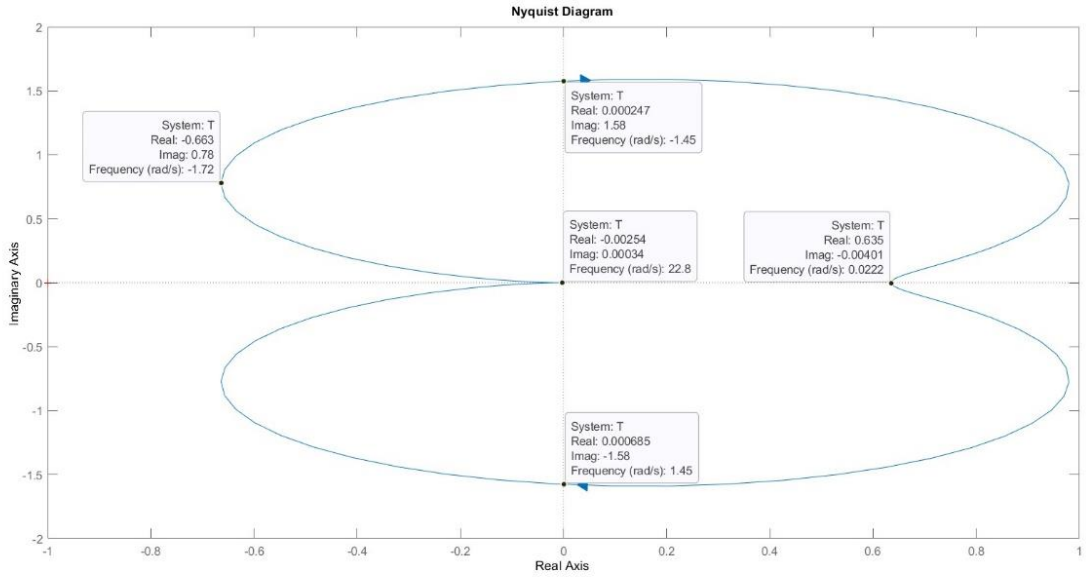

Figure 15: Nyquist Plot – Poles and Gains

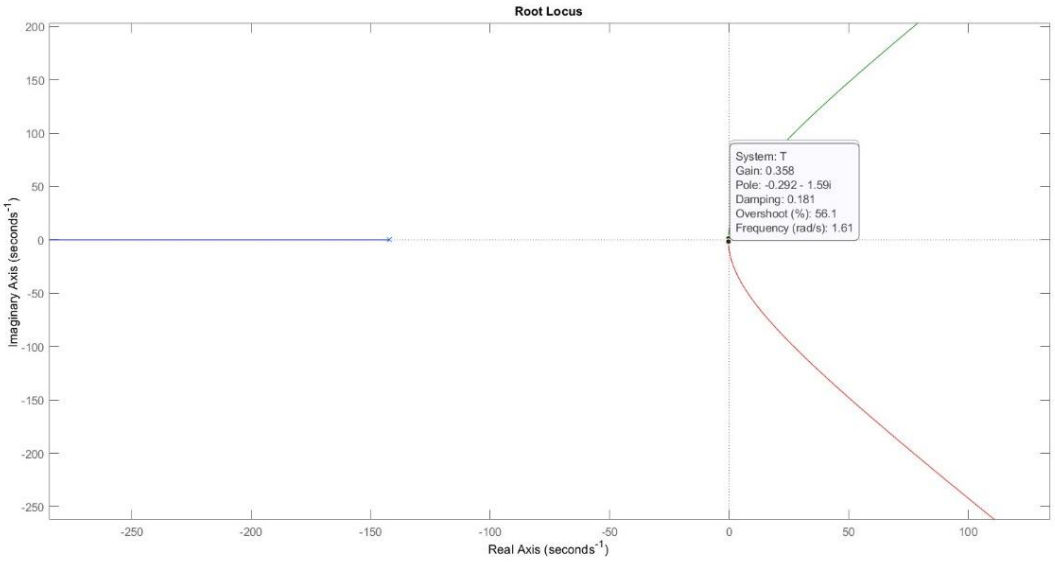

Figure 16: Root Locus Plot

Figure 17: Root Locus - Poles and Gains

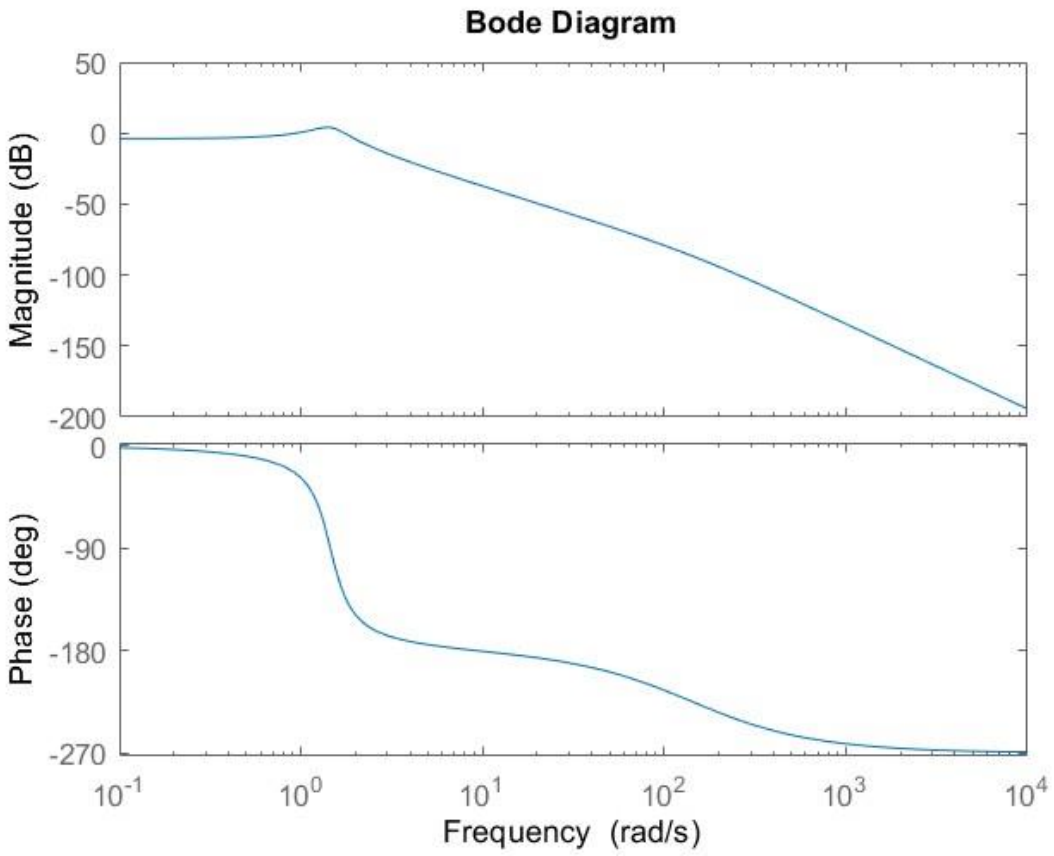

Figure 18: Bode Diagram

3.3. Control Implications

Designing and applying a controller ensures that the solar tracker system achieves the performance specifications outlined in Table 1 in section 1. A controller could however be rendered unnecessary by using a gearbox with a gear ratio that is high enough to ensure that the solar tracker system moves at the same speed as the sun which would ensure perfect tracking.

This means that the motor would have to run continuously throughout the day which has adverse effects on the life of the system, and without control it would mean that the system would have no means of accounting for disturbances.

4. Controller Design

The system is required to have no steady state error. This meant that a proportional control mode would not be sufficient as it cannot eliminate the errors. A PI control mode was determined to be more appropriate as the incorporation of the integral control meant that the

steady state error of the system could be improved, and it is less costly to implement when compared to a full PID control mode.

4.1. PI control design

The manipulated output for the PI mode of control is show in equation…. below.

$$V(s) = \left(K_P + \frac{K_I}{s}\right) E(s)$$

The K_P and K_I gains had to be determined and this was done using two methods. The methods are the manual input of various K_P and K_I gain values using the PID function in MATLAB and applying PI control the system and visualising the response along with the response performance parameters, the other method is the automatic PID tuning in Simulink.

4.1.1. Manual tuning

The value of the K_P was determined first, with respect to the system performance goals. The value was initially set to one and then increased by an order of magnitude until the value of one hundred.

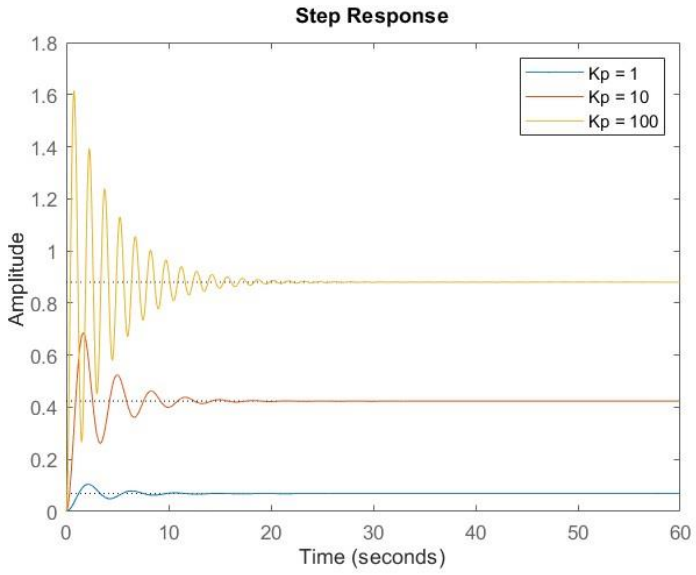

Figure 19:Response to various KP gains.

Figure 18 shows that the system response exhibited a smaller steady state error with reference to the amplitude value of one, however, it overshot past that value which violated the performance goal of a step response with zero percentage overshoot. The K_P gain value of ten did not overshoot past the amplitude value, however, it had a larger settling time as observed

in Figure 18. The K_P gain value of one was determined to be better suited for system as it had smaller oscillations and a faster settling time.

The K_I gain value was tuned to suit the K_P gain of one. The K_I gain value was initially set to a value of one and then increased by one until the value of three.

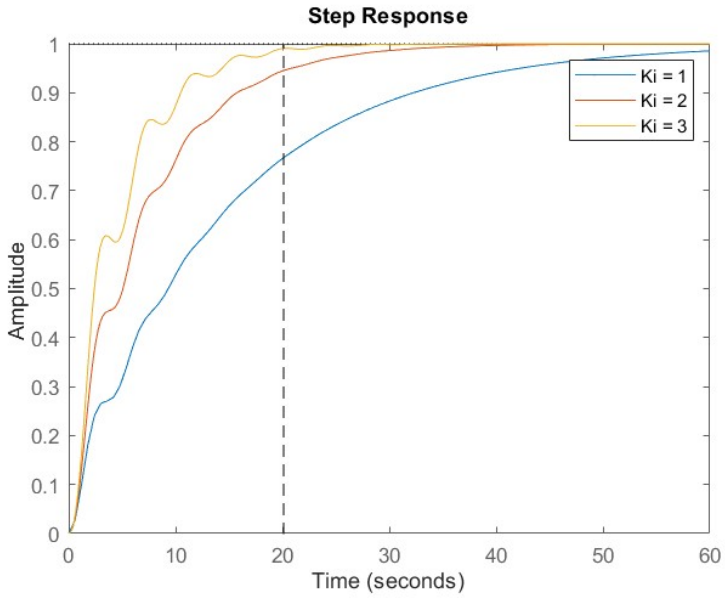

Figure 20: Response to various K_I gains with $K_P = 1$.

Figure 8 shows the system response to various K_I when K_P was set to one. The combination of a K_P gain value of one and a K_I gain value three met the system performance goals. The performance specifications of the combination are summarized in table… below.

Table 4: Performance specification with $K_P = 1$ and $K_I = 3$.

Performance specification	Value
Rise time	9.5 seconds
Settling time	18.7 seconds
% Overshoot	0 %
Peak value	1

4.1.2. Simulink Tuning

The PID controller design was completed in Simulink to facilitate control of the system. To achieve this, PID tuning was used through the Simulink 'ControlSystemDesigner' interface. The resulting gains and system performance are show in table 5 below.

Table 5: PID tuner results.

Parameter specifications	Value

K_P	0.83
K_I	2.85
Rise time	9.78 seconds
Settling time	19.1 seconds
% Overshoot	0 %
Peak value	1

The gains obtained the Simulink PID tuner are close to the ones that were obtained by manually trying different combinations of K_P and K_I using engineering judgement. The gains obtained through the PID tuner are the ones that were used to control the system.

The response of the uncontrolled system and the PI controlled system to a unit step input are shown in figure 15 below. The controlled system meets the performance specification goals for this application.

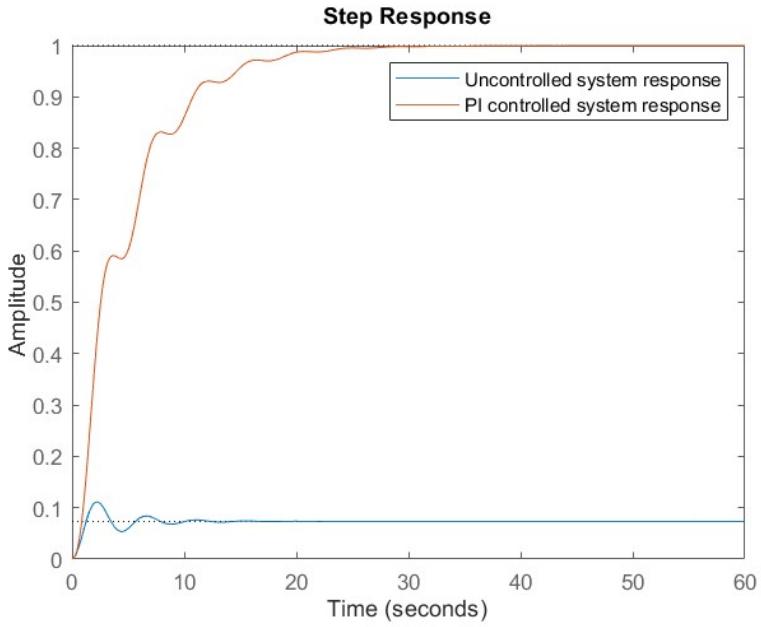

Figure 21: Comparison of controlled and uncontrolled system response.

4.2. Root-locus technique

Upon establishing the systems need for control. The system's robustness was investigated, as it can help show the sensitivity of the system. As for this design it, involves using the stability of the in the presence of changing system input which is the required panel position. This indicates that the system's state at each point the panel tracks the sun is not the same. This is

inherently due the type loads the gears experience to keep the panel fixed and the initial torque needed to ensure the required amount of rotation matching the required sun position is met.

This sensitivity was investigated using a root locus of the open loop transfer function. It shows how the poles vary with varying inputs. This information would need to be known, to know what the limitation toward the system's stability. It also defines the range of stability for gain values that are to act on the transfer function. Thus, enabling insight on how to select controller gains. Then the root locus was further used to define the limiting stability point of gain inputs at varying inputs. Thus, reduce time in establishing control gains needed to ensure the system meet performance parameters.

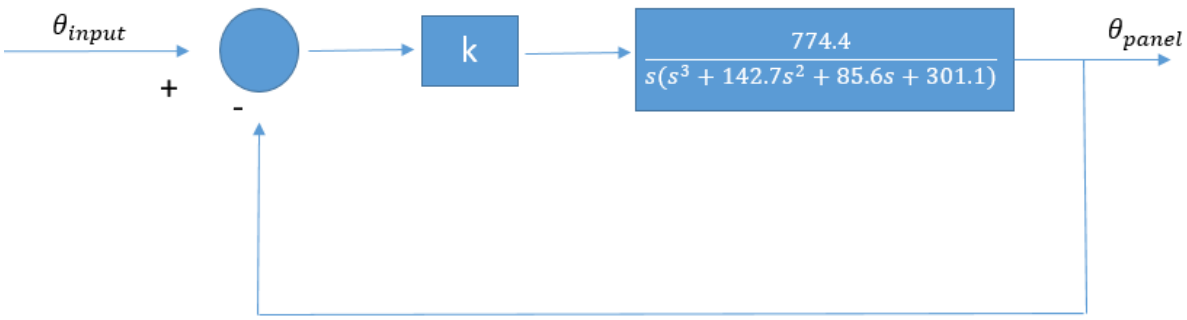

Figure 22 showing the block diagram representation of the k gain acting imposed on the transfer function

Then the root locus was analysed using

$$G(s) = \frac{774.4k}{(s^3 + 142.7s^2 + 85.6s + 301.1)} = \frac{N(s)}{D(s)}$$

Whereby the denominator was used equated to zero in order to find the poles as by inspection they are no zeros from the numerator and there are three poles. Which are

s = -133.3 ; $\pm$j0.95 from $s^3 + 142.7s^2 + 85.6s + 301.1 = 0$

The break way point is a point on the real axis where the poles converge and diverge with k varying. The location of the break way can inform on how the sensitive the system is to change input and disturbance. As the closer to the origin from the left side of the Im axis the more sensitive the system is to change.

Using $1 + G(s)H(s) = 0$ which is $\frac{d}{ds}(s^3 + 142.7s^2 + 85.6s) = 0$

The possible break way points are $s = -0.302\ and\ -94{,}49$. The final break way location for the system is $s = -0.302$ this is due to it having dominant effect over $-94{,}49$ for the system's response. This was assessed using dominant root analysis.

Then asymptotes were established. As they show the path of the poles and were they are trending to on a long term. In that regard the asymptotes allow for the prediction of the poles over a long term as k approaches a certain gain value. The angles were found using

Angle $= \frac{(2k+1)180}{n-m}, k = 0,1,2,3 \ldots$ which gave $\theta_0 = 60°$. Only θ_0 was comput4ed for because we investigating the gain k limit range and behaviour which require the asymptotes that show the extreme location of varying poles.

The asymptotes intersecting the real axis is through:

$$\sigma_a = \frac{\Sigma poles - \Sigma zeros}{n-m} = -\frac{133.3}{3} = 44.43.$$

As this position informs on how sensitive the system to changes in k and poles. Whether is large interval that k can vary with poles varying without resulting in the system being unstable. After defining the aspects of the root locus for this system. It was then drawn which what is shown in figure 16.

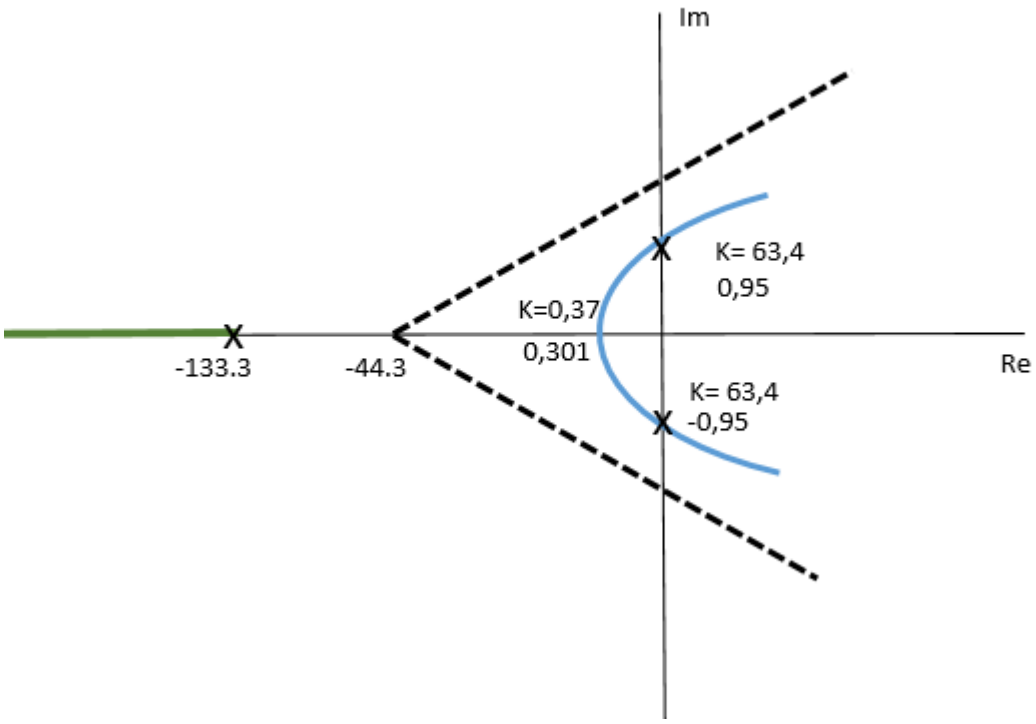

Figure 23 showing the root locus analytically drawn not to scale.

Observing from the root locus it is evident that the system is stable but sensitive to the changes that may occur during the response. This is due to the break way being close to the imaginary axis. This further shows that there less poles for varying the gain k the system will be stable hence it susceptible to disturbance. Then observing that it has complex root by the transfer

function. The system will show underdamped behaviour that will cause oscillatory behaviour which what was observed in the response. This shows that system is critically stable for small ranges of poles and gain and has robust.

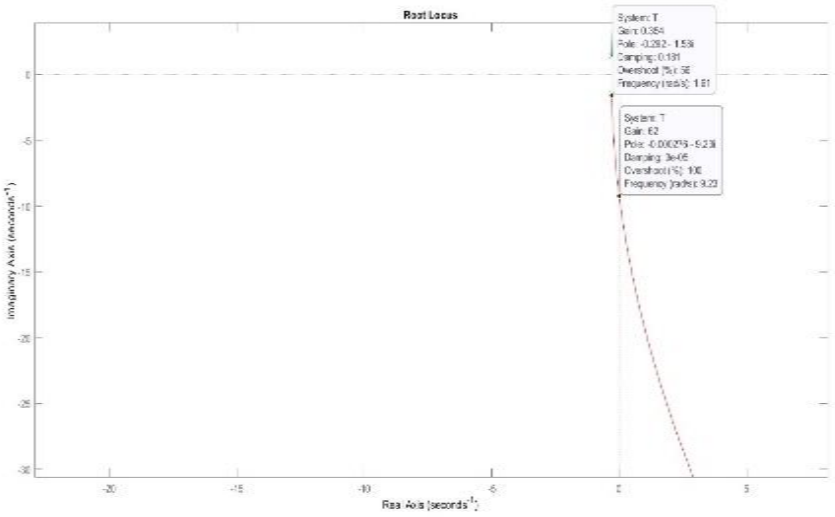

Figure 24 showing the root locus from MATLAB.

To validate the root locus computed analytically, a root locus of the transfer function using MATLAB was developed. This root locus showed to exhibit the same behaviour and k gain values were similar with little variation. Showing that the root locus developed in figure 21 informs about the system precisely.

Nyquist Plot

The Nyquist plot is used to observe how the system behaves with changes in frequency, over a response. It accounts for delay time which is inherent in the how the response changes. Which is why it considered despite performing the root locus. The Nyquist inform on the systems stability, which is when -1 is not enclosed and the changes in frequency are more likely to push the system an unstable state.

The Nyquist equation was derived using the transfer function:

$$T(S)\frac{774.4}{(s^3 + 142.7s^2 + 85.6s + 301.1)}$$

Whereby s = $j\omega$ which results in:

$$T(j\omega)\frac{774.4}{((j\omega)^3 + 142.7(j\omega)^2 + 85.6(j\omega) + 301.1)}$$

This e

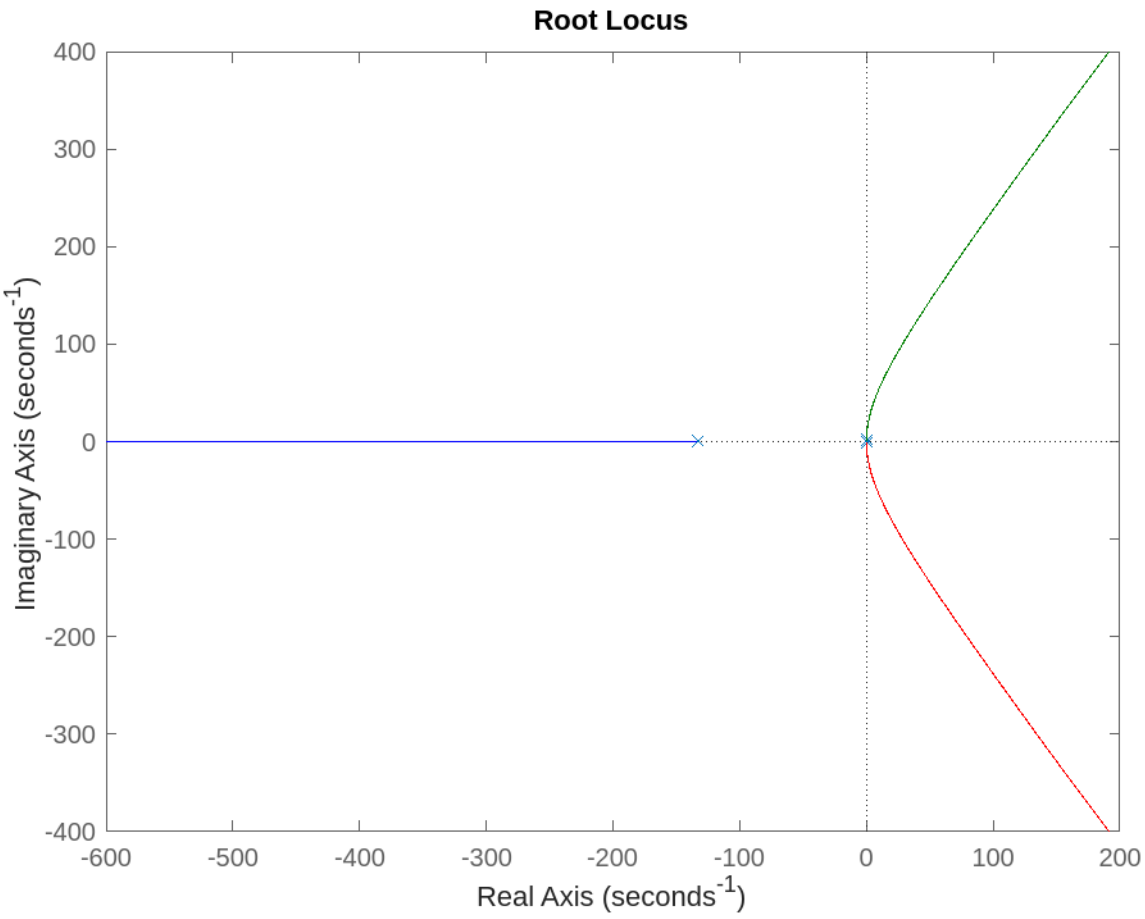

5. System evaluation

5.1. Analytical evaluation

The application of a Proportional and integral controller gains resulted in the following closed loop system transfer function.

$$\frac{\Theta_P(s)}{\Theta_S(s)} = \frac{18.36s + 63.04}{s^4 + 142.7s^3 + 85.6s^2 + 319.5s + 63.04}$$

The system stability was analysed using the Routh Hurwitz stability criterion. The Routh Hurwitz array is show in table 5. The first column has no sign change which indicates that system has no roots in the right-hand plane and is thus stable.

Table 6: Routh Hurwitz array for the controlled system

s^4	1	85.6	63.04
s^3	142.7	319.5	0
s^2	83.36	141.144	
s^1	77.88	0	
s^0	141.144		

The system's steady state error in response to a step input was determined next. The open loop transfer function was as follows.

$$\frac{\Theta_P(s)}{\Theta_S(s)} = \frac{18.36s + 63.04}{s^4 + 142.7s^3 + 85.6s^2 + 301.1s}$$

Applying the static error constants equation for a ramp input to the open loop transfer function resulted in a steady state error of zero. This shows that the system is controlled and responds to the step input as desired.

5.2. Simulation evaluation

The simulation was used to output the bode plot shown in figure 18. The bode plot shows that the system has a gain margin of 9.31 dB at the frequency of 1.66 rad/s and a phase margin of 178.88° at the frequency of 0.0041 rad/s.

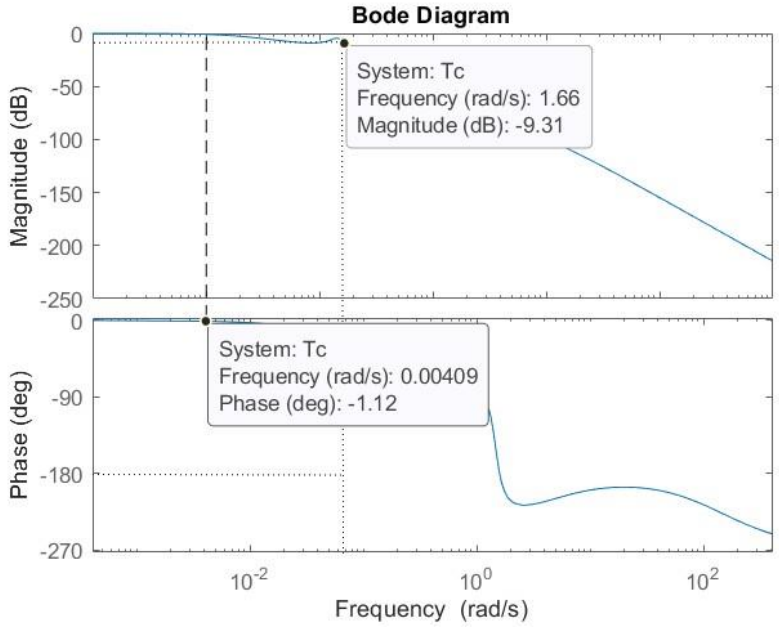

Figure 25: Bode plot for the controlled system.

5.3. Response to sun position input

The main purpose of the design was to create a solar tracker that could maximise sun absorption by following the path of the sun as it moves across the sky. The panel makes use of a single axis tracker that follows the sun's position at various times throughout each day.

The data for the sun's position at various times of the year was obtained from solar tracking sources, The data obtained is attached in the appendix. The Simulink model was set up to ensure the designed model could track the sun's position even in the presence of a disturbance. A step input disturbance was inserted to show the effect of a sudden wind gust on the panel at a point in time.

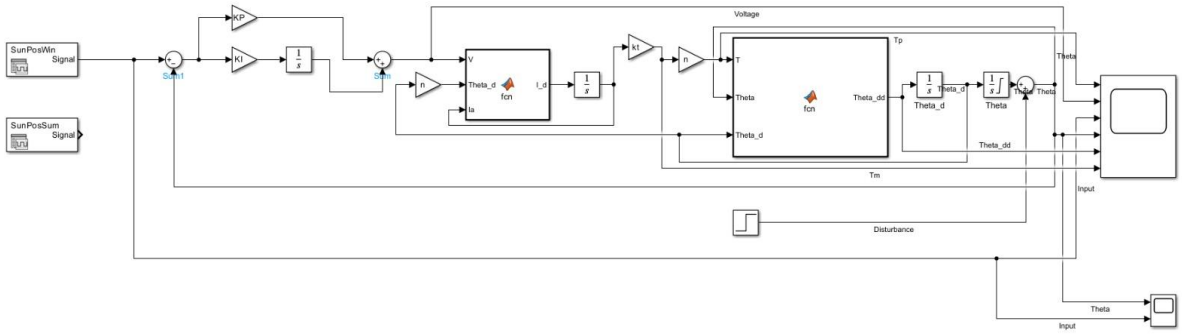

Figure 26: Sun position tracker model.

The model was designed such that it could operate for any day of the year, regardless of the season and sun trajectory. To demonstrate this response, the system was modelled during peak summer conditions and peak winter conditions where the suns position would be at its highest and lowest respectively.

As seen in Figure 27, the sun's position during summer is significantly higher and as a result requires higher turn angle limits. Regardless of the season, the tracker potion can match the sun's input position relative to the tracker. The lack of oscillations is attributed to the performance parameters that were set through the design of the controller. The system has a low overshoot and large settling time to

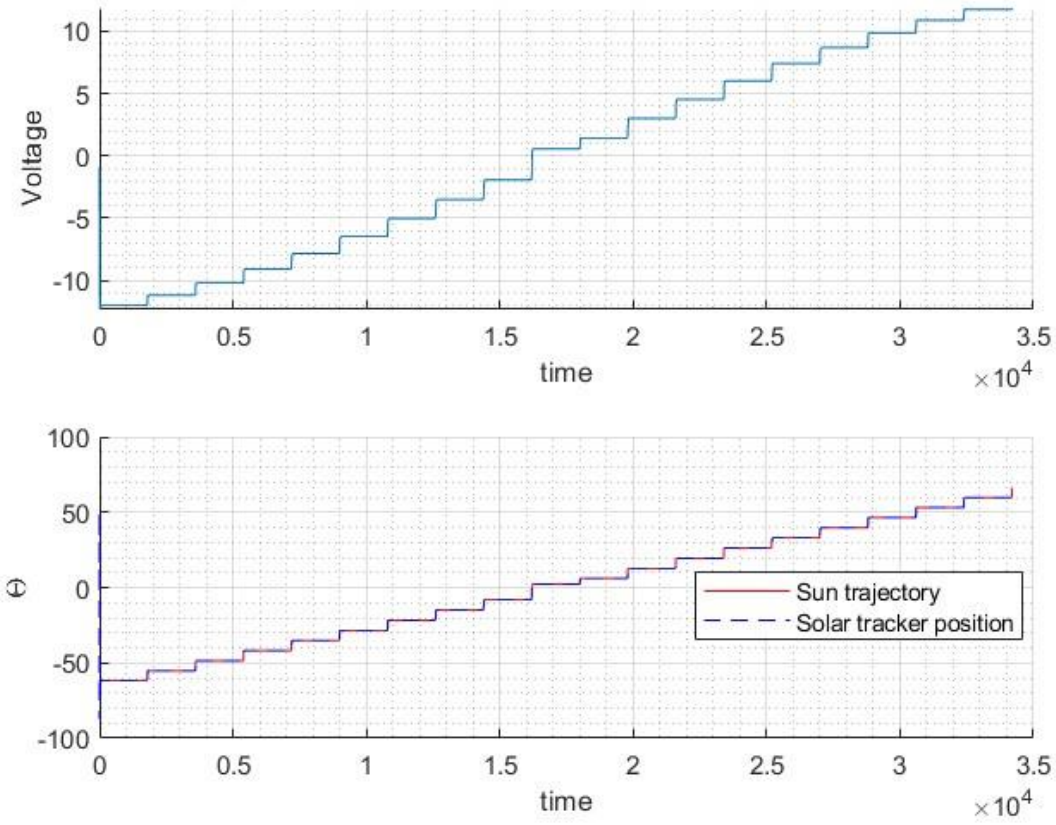

Figure 27: Summer tracking

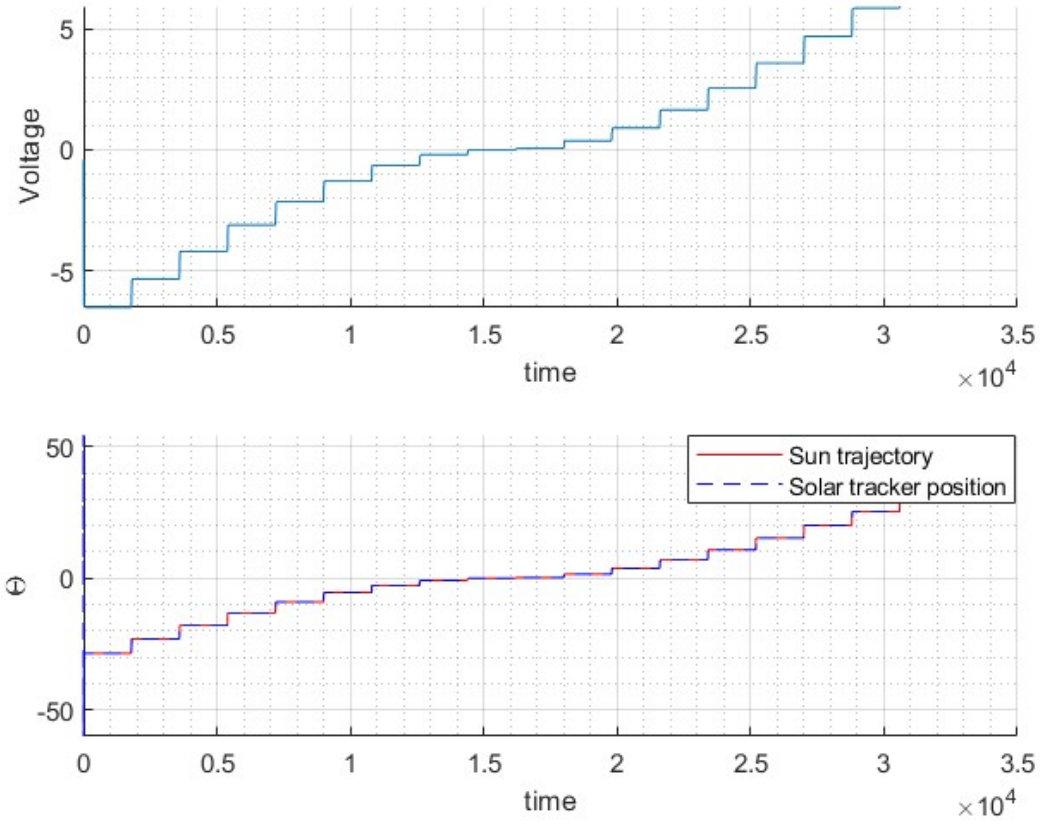

Figure 28: Winter tracking

6. Recommendations

For optimal sunlight absorption, it is recommended that the solar tracker be designed for both the azimuth and zenith axis. Despite the systems ability to track the sun's position daily, the relative tilt of the sun will change throughout the year. The current model assumes the suns position to move directly about the axis of rotation (i.e the sun rays are perpendicular to the panel asit moves).

Bibliography

Nice, N. s., 2010. *Control systems engineering.* aNew York: Wiley.

SunEarthTools, 2024. *Tools for consumers and designers of solar.* [Online] Available at: https://www.sunearthtools.com/dp/tools/pos_sun.php#annual [Accessed 19 April 2024].

https://gosunbolt.com/workstations/campusxl/